

Photoluminescence Properties of Eu^{2+} in BaB_2O_4 A.B. Gawande¹, R.P. Sonekar^{2,*} and S.K. Omanwar¹¹Department of Physics, SGB Amravati University, Amravati-444602 (M.S.), India.²Department of Physics, G.S. College, Khamgaon, Dist: Buldhana (M.S.), India.

ARTICLE INFO

Article history:

Received: 9 December 2013;

Received in revised form:

15 October 2014;

Accepted: 28 October 2014;

Keywords

Borate,
Combustion synthesis,
UV emitter,
Photoluminescence.

ABSTRACT

The photoluminescence properties of Eu^{2+} doped BaB_2O_4 prepared by novel solution combustion synthesis technique are investigated. The structure of the prepared sample characterized by TG-DTA, XRD and FTIR. Surface morphological study was done using SEM images. $\text{BaB}_2\text{O}_4:\text{Eu}^{2+}$ gives strong emission at 380 nm (UV-A region), upon excitation with 322 nm light. The concentration of Eu^{2+} (relative to Ba) in BaB_2O_4 for which the quenching occur was found to be about 6 mol%, and the critical transfer distance for this concentration was calculated to be 14.56 Å. This phosphor may provide an efficient kind of luminescent material for various applications in medical & industry.

© 2014 Elixir All rights reserved

Introduction

Since about 40 years the use of UV radiation for phototherapy is well established. UVR has many uses as a natural source of energy and is important in various biological processes. Artificial sources of UVR are used for tanning, medical diagnosis and treatment, and promoting polymerization reactions. Exposure to UVR usually is expressed as a dose rate in watts per square meter (the power striking a unit surface area of an irradiated object). The commonly used unit of effective dose is the minimal erythema dose (MED), which is defined as the lowest radiant exposure to UVR sufficient to produce erythema of the skin with sharp margins within 24 hours of exposure. Though imprecise, MEDs are useful, because they are related to the biological consequences of the exposure (IARC 1992). Many phosphor emits UVR (UVA, UVB & UVC) upon excited by suitable wavelength light which are commercially using for treating about 40 types of skin diseases and disorders (1-17). Photo luminescent materials including oxides, silicates, aluminates, aluminoborates, aluminosilicates, nitrides, borates etc., plays a very important role for the potential applications in ultraviolet devices. Among these hosts investigated, borates are good candidates as hosts due to their low synthetic temperature, easy preparation and high luminescent brightness. The luminescence properties of Eu^{2+} ions in alkaline earth haloborates [18], and in SrB_4O_7 [19] have been investigated by some researchers.

In this paper we have reported the photoluminescence properties of an alkaline earth borate BaB_2O_4 doped with Eu^{2+} , prepared by novel solution combustion synthesis method.

Material and Method

Inorganic borate phosphors were prepared by a novel method described earlier [20-22], which is a variation of the combustion synthesis. The method based on exothermic reaction in which ammonium nitrate used as oxidizer and urea is used as fuel. Fig.1 shows the stepwise preparation of samples by using combustion synthesis technique. The stoichiometric amounts of high purity starting materials, $\text{Ba}(\text{NO}_3)_2$ (A.R.), Eu_2O_3 (high purity 99.9%), H_3BO_3 (A.R.), $\text{CO}(\text{NH}_2)_2$ (A.R.), NH_4NO_3 (A.R.)

have been used for sample preparation. The starting materials with little amount of DD water were mixed thoroughly in agate mortar to obtain homogeneous solution.

The excess water has been removed by slow heating (70°C) and the solution then transferred directly to the pre-heated furnace (550°C) for combustion. Following the combustion, the resulting foamy sample were crushed to obtain fine particles and then annealed for 4 hr at temperature 800°C under reducing atmosphere. The prepared material were characterized by powder XRD and FT-IR. Powder X-ray diffraction measurement were taken on Rigaku Miniflex X-ray Diffractometer and compared with the ICDD file. Morphology and size of the calcined particles were observed by scanning electron microscopy (SEM). PL & PLE measurements at room temperature were performed on Hitachi F-7000 spectrophotometer in the range 200–500 nm with spectral resolution of 2.5 nm and PMT voltage of 400 Volts.

Table: Molar ratio of ingredients used for material preparation

Compound	Molar Ratio
$\text{Ba}_{(1-x)}\text{Eu}_x\text{B}_2\text{O}_4$	$\text{Ba}(\text{NO}_3)_2 : \text{Eu}(\text{NO}_3)_2 :$ $\text{H}_3\text{BO}_3 : \text{CO}(\text{NH}_2)_2 : \text{NH}_4\text{NO}_3$ (1-x) : x : 2 : 3 : 4 (x = 0.03, 0.04, 0.05, 0.06, 0.07, 0.08)

Result and Discussion

TG-DTA Analysis

Decomposition of the $\text{Ba}_{(1-0.94)}\text{B}_2\text{O}_4:\text{Eu}_{0.06}$ precursors and the subsequent phase formation process monitored by TG-DTA are shown in Fig. 1.

About less than 0.5% weight loss is observed in the TG curve of the precursor within the range of 40 to 170°C , indicating evaporation constituted water molecules. The main weight loss of about 2% is observed in the range 200 - 620°C , which agrees with the first endothermic peak (DTA curve) caused by the evaporation of organic solvent, decomposition of nitrates and boric acid. No obvious weight loss after 800°C indicates that BaB_2O_4 can be formed at around 800°C .

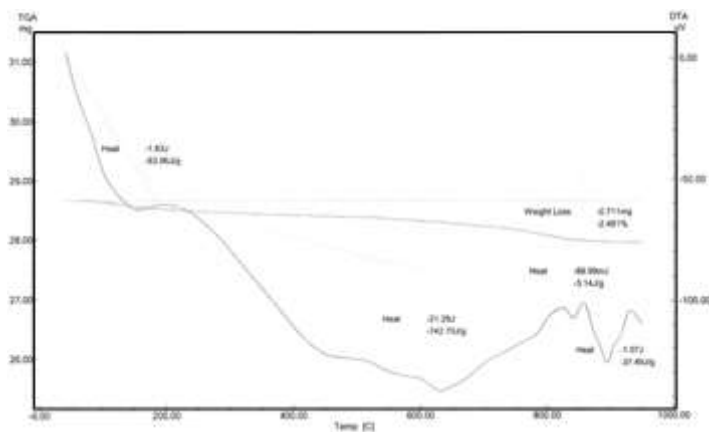


Fig 1: TG-DTA analysis results of the $\text{Ba}_{(1-0.94)}\text{B}_2\text{O}_4:\text{Eu}_{0.06}$ precursor (Heating rate: $50^\circ\text{C}/\text{min}$; Gas flow: air)

X-ray Diffraction Pattern

The powder XRD pattern of BaB_2O_4 (Fig.1), compared with ICDD file no. 00-024-0086 and found consistent with reference [24]. The crystal structure of the prepared BaB_2O_4 can be refined to be monoclinic, space group $C2/c$ with $a = 11.133 \text{ \AA}$, $b = 12.67 \text{ \AA}$ and $c = 8.381 \text{ \AA}$. It is different from the reported $\beta\text{-BaB}_2\text{O}_4$, which is rhombohedral, space group $R3c$ with $a = b = 12.532 \text{ \AA}$ and $c = 12.726 \text{ \AA}$, (PDF#38-0722) [23, 24].

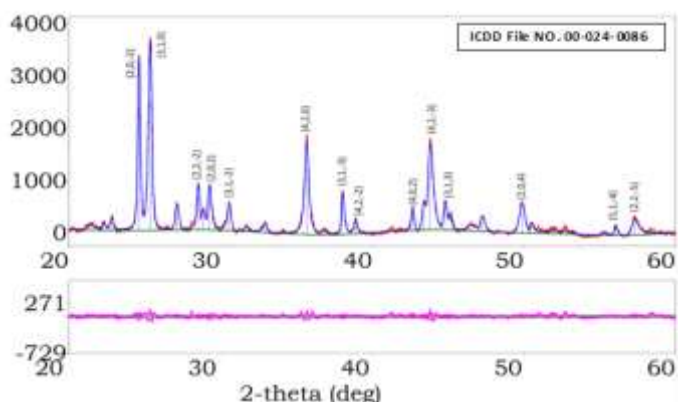


Fig 2: The X-ray powder diffraction patterns of $\text{Ba}_{0.94}\text{B}_2\text{O}_4:\text{Eu}_{0.06}^{2+}$.

SEM image of phosphor powder

Fig. 3 shows the SEM image of $\text{Ba}_{0.94}\text{B}_2\text{O}_4:\text{Eu}_{0.06}^{2+}$ powder prepared at 800°C . It was observed that the microstructure of the phosphor consisted of irregular grains with heavy agglomerate phenomena. The average size of the $\text{Ba}_{0.94}\text{B}_2\text{O}_4:\text{Eu}_{0.06}^{2+}$ particles is about $4\text{--}10 \mu\text{m}$. The results show that $\text{BaB}_2\text{O}_4:\text{Eu}^{2+}$ phosphor has a good crystallinity and a relatively low sinter temperature.

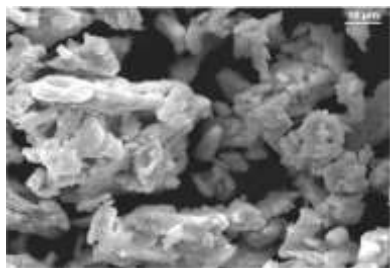


Fig 3: SEM image of $\text{Ba}_{0.94}\text{B}_2\text{O}_4:\text{Eu}_{0.06}^{2+}$.

Photoluminescence of $\text{BaB}_2\text{O}_4:\text{Eu}^{2+}$

The excitation and emission spectra of $\text{Ba}_{0.94}\text{Eu}_{0.06}\text{B}_2\text{O}_4$ are shown in Fig.4. The $^8\text{S}_{7/2}$ state with the $4f^7$ configuration is the ground state of the Eu^{2+} ion. Within this configuration, the $^6\text{P}_j$ states are the excited state with the lowest energy [25]. The excited states of Eu^{2+} may be formed from the $4f^65d$ configuration; the crystal field causes a splitting of the $4f^65d$

configuration of the Eu^{2+} ion in the phosphors. Therefore the lowest excited state is below the $^6\text{P}_j$ state and only $4f^7(^8\text{S}_{7/2})$ to $4f^65d$ transitions within the Eu^{2+} ions are observed in excitation and emission [26]. The emission spectrum observed in the present work at 380 nm . This emission band corresponds to the $4f^7 \rightarrow 4f^65d$ transition which strongly depends on the anion environment around Eu^{2+} ion. The excitation spectrum at 322 nm and other weak bands in the ultraviolet region are assigned to the electric dipole allowed transitions. The effect of doped Eu^{2+} concentration on the emission of $\text{BaB}_2\text{O}_4:\text{Eu}^{2+}$ phosphor was also investigated. The emission and excitation spectra of $\text{BaB}_2\text{O}_4:\text{Eu}^{2+}$ phosphors prepared at various concentrations of Eu^{2+} ($x = 0.03, 0.04, 0.05, 0.06, 0.07, 0.08$) are shown in Fig.4 & Fig.5. The PL intensity increases with Eu^{2+} concentration increasing until a maximum intensity is reached, and then it decreases due to concentration quenching. From Fig.5, we can see that the critical concentration quenching (χ_c) of Eu^{2+} in $\text{BaB}_2\text{O}_4:\text{Eu}^{2+}$ phosphor is about 6 mol%. According to Blasse [27], for the critical concentration the average shortest distance between nearest activator ions is equal to the critical distance R_0 . R_0 is, in fact, the critical separation between donor (activator ion) and acceptor (quenching ion), at which the nonradiative rate equals that of the internal single ion relaxation. The R_0 value can be practically calculated using the following equation.

$$R_0 = 2 \times \left(\frac{3V}{4\pi\chi_c N} \right)^{1/3}$$

Where, χ_c is the critical concentration, N the number of Ba^{2+} ions in the BaB_2O_4 unit cell, and V the volume of the unit cell. By taking the experimental and analytic values of χ_c , N and V (0.06 , 12 and 1164.12 \AA^3 , respectively), the critical transfer distance R_0 for $\text{BaB}_2\text{O}_4:\text{Eu}^{2+}$ was determined to be about 14.56 \AA .

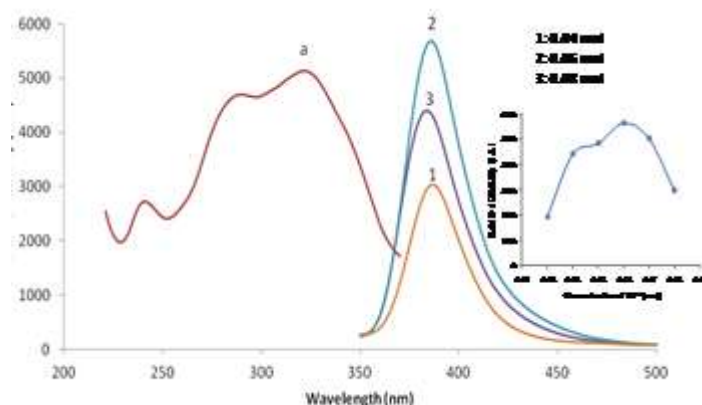


Fig 4: Excitation (a) and Emission (1: 0.04, 2: 0.06, 3: 0.08) of Eu_x^{2+} in $\text{Ba}_{(1-x)}\text{B}_2\text{O}_4$, ($x=0.04, 0.06, 0.08$).

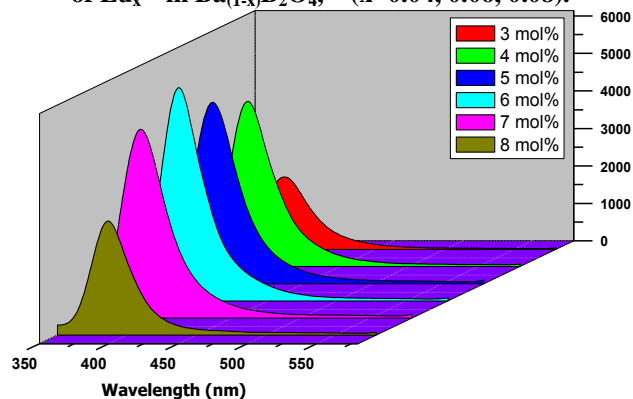


Fig 5: Variation in emission intensity of Eu_x^{2+} in $\text{Ba}_{(1-x)}\text{B}_2\text{O}_4$, ($x=0.03, 0.04, 0.05, 0.06, 0.07, 0.08$).

Conclusion

In this work, we prepared some new UV emitting phosphors $\text{BaB}_2\text{O}_4:\text{Eu}^{2+}$ by using solution combustion technique and its photoluminescence properties were reported. TG-DTA study supports to the formation of various phases of BaB_2O_4 in the range 40 – 950 °C. The structure conformation as synthesized phosphor was characterized by using powder XRD technique. FT-IR spectroscopy conforms the existence of the $[\text{BO}_3]^{3-}$ groups. The SEM image represents the formation of irregular shape particles. of calcined powder for 4 hr indicated highly agglomerated powders. The phosphor $\text{BaB}_2\text{O}_4:\text{Eu}^{2+}$ give emission at 380 nm upon excited by 322 nm wavelength. It is also found that the concentration of Eu^{2+} (relative to Ba) in BaB_2O_4 for which the quenching occur is 6 mol%, and the critical transfer distance for this concentration was calculated to be 14.56 Å. The phosphor may provide the efficient candidate for various applications in medical and industry.

References

- [1] Honigsmann H, Brenner W, Rauschmeier W. *J. Am. Acad. Dermatol* 1984;10: 238-245.
- [2] Scherschun L, Kim JJ, Lim WH. Narrow-band ultraviolet B is a useful and well-tolerated treatment for vitiligo. *J Am Acad Dermatol* 2001;44: 999-1003.
- [3] Ota T, Hata Y, Tanikawa A, Amagai M, Tanaka M, Nishikawa T. Eosinophilic pustular folliculitis (Ofuji's disease): indomethacin as a first choice of treatment. *Clin Exp Dermatol* 2001;26: 179-181.
- [4] Warren LJ, George S. Erythropoietic protoporphyria treated with narrow-band (TL-01) UVB phototherapy. *J Australas Dermatol* 1998;39: 79-182.
- [5] Enk CD, Elad S, Vexler A, Kapelushnik J, Gorodetsky R, Kirschbaum M. Chronic graft-versus-host disease treated with UVB phototherapy. *Bone Mar Tr* 1998;22(12): 1179-1183.
- [6] Leenutaphong V, Jiamton S. UVB phototherapy for pityriasis rosea: a bilateral comparison study. *J Am Acad Dermatol* 1995;33: 996-999.
- [7] Blachley JD, Blankenship DM, Menter A, Parker TF, Knochel JP. Uremic pruritus: skin divalent ion content and response to ultraviolet phototherapy. *Am J Kidney Dis* 1985;5: 237-241.
- [8] Dittmar HC, Pflieger D, Schopf E, Simon JC. UVA1 phototherapy: Pilot study of dose finding in acute exacerbated atopic dermatitis. *Hautarzt* 2001;52: 423-427.
- [9] Kreuter A, Jansen T, Stucker M, Herde M, Hoffmann K. Low-dose ultraviolet-A1 phototherapy for lichen sclerosus et atrophicus. *Dermatol* 2001;26: 30-32.
- [10] Gruss CJ, von Kobyletzki G, Behrens-Williams SC, Lininger J, Reuther T, Kerscher M, Altmeyer P. Effects of low dose ultraviolet A-1 phototherapy on morphea. *Photodermatol Photoimmunol Photomed* 2001;17(4): 149-155.
- [11] Morita A, Kobayashi K, Isomura I, Tsuji T, Krutmann J. Ultraviolet A1 (340-400 nm) phototherapy for scleroderma in systemic sclerosis. *J Am Acad Dermatol* 2000;43: 670-674.
- [12] Plettenberg H, Stege H, Megahed M, Ruzicka T, Hosokawa Y, Tsuji T, Morita A, Krutmann J. Ultraviolet A1 (340-400 nm) phototherapy for cutaneous T-cell lymphoma. *J Acad Dermatol* 1999;41: 47-50.
- [13] Millard TP, Hawk JLM. Ultraviolet therapy in lupus. *Lupus* 2001;10(7): 185-187.
- [14] Wiskemann AZ. UVB-Phototherapie der Psoriasis mit einer für die PUVA-Therapie entwickelten Stehbox. *Z Hautkr* 1978;53: 633-666.
- [15] Pathak A Madhukar and Thomas B Fitzpatrick. The evolution of photochemotherapy with psoralens and UVA (PUVA): 2000 BC to 1992 AD. *J Photochem Photobiol B: Biology* 1992;14: 3-22.
- [16] Mcgrath H, Bell JM, Haynes MR, Martinezosuna P. Ultraviolet-A Irradiation Therapy for Patients with Systemic Lupus-Erythematosus - A Pilot-Study. *Current therapeutic research* 1994;55(4): 373-381.
- [17] Zanolli Michael. Phototherapy treatment of psoriasis today. *J Am Acad Aematol* 2003;49: S78-S86.
- [18] Peters TE, Baglio J. Luminescence and structural properties of alkaline earth chloroborates activated with divalent europium. *J Inorg Nucl Chem* 1971;32: 1089-1095.
- [19] Stefani R, Maia AS, Kodaira CA, Teotonio EES, Felinto MCFC, Brito HF. Highly enhanced luminescence of $\text{SrB}_4\text{O}_7:\text{Eu}^{2+}$ phosphor prepared by the combustion method using glycine as fuel. *Opt Mater* 2007;29: 1852–1855.
- [20] Sonekar RP, Omanwar SK, Moharil SV, Dhopte SM, Muthal PL, Kondawar VK. Combustion synthesis of narrow UVB emitting rare earth borate phosphors. *Opt Mater* 2007;30: 622–625.
- [21] Sonekar RP, Omanwar SK, Moharil, Muthal PL, Dhopte SM, Kondawar VK. Luminescence in $\text{LaBa}_9\text{O}_{16}$ prepared by combustion synthesis. *J Lumin* 2006;129(6): 624-628.
- [22] Kingsley JJ, Suresh K, Patil KC. Combustion synthesis of fine particle metal aluminates. *J Mater Sci* 1990;25: 1305-1312.
- [23] Zou WG, Lü MK, Gu F, Xiu ZL, Wang SF, Zhou GJ. Luminescence properties of Eu^{3+} and Dy^{3+} doped $\beta\text{-BaB}_2\text{O}_4$ nanocrystals. *Opt Mater* 2006;28: 988–991.
- [24] Liu Jie, Wang Xiang-De, Wu Zhan-Chao, Kuang Shao-Ping. Preparation, characterization and photoluminescence properties of $\text{BaB}_2\text{O}_4:\text{Eu}^{3+}$ red phosphor. *Spectrochimica Acta Part A* 2011;79: 1520-1523.
- [25] Toderas M, Filip S, Ardelean I. Structural study of the $\text{Fe}_2\text{O}_3\text{-B}_2\text{O}_3\text{-BaO}$ glass system by FTIR spectroscopy. *J Optoelectron Adv Mater* 2006;8: 1118–1120.
- [26] Motke SG, Yawale SP, Yawale SS. Infrared spectra of zinc doped lead borate glasses. *Bull Mater Sci* 2002;25(1): 75–78.
- [27] Blasse G. Energy transfer in oxidic phosphors. *Philips Res Rep* 1969;24: 131–144.